

Cite this article as: Sun Qiancheng, Yao Qingrong, Long Qianxin, et al. Effect of Adding $\text{Ho}_{63.3}\text{Fe}_{36.7}$ to Grain Boundaries on Structure and Properties of Regenerated NdFeB Magnets[J]. Rare Metal Materials and Engineering, 2021, 50(12): 4230-4235.

ARTICLE

Effect of Adding $\text{Ho}_{63.3}\text{Fe}_{36.7}$ to Grain Boundaries on Structure and Properties of Regenerated NdFeB Magnets

Sun Qiancheng¹, Yao Qingrong¹, Long Qianxin¹, Huang Weichao², Deng Jianqiu¹, Wang Jiang¹, Rao Guanghui¹, Zhou Huaiying¹

¹ Guangxi Key Laboratory of Information Materials, School of Materials Science and Engineering, Guilin University of Electronic Technology, Guilin 541004, China; ² China Rare Metals and Rare Earth (Guangxi) Jinyuan New Materials Co., Ltd, Hezhou 542603, China

Abstract: A high-efficiency and green physical method was proposed to clean the surface of NdFeB waste magnets for recycling. NdFeB regenerated magnets were fabricated by adding low-melting point $\text{Ho}_{63.3}\text{Fe}_{36.7}$ alloy to grain boundaries. Results show that in magnets without $\text{Ho}_{63.3}\text{Fe}_{36.7}$, there are insufficient Nd-rich phases to isolate the $\text{Nd}_2\text{Fe}_{14}\text{B}$ phase, leading to poor magnet performance. With the addition of $\text{Ho}_{63.3}\text{Fe}_{36.7}$ alloy, the grain boundary phases become clear and concatenated. Optimal magnetic energy $[(BH)_{\max} + H_{\text{ci}} = 1756.07]$ can be obtained by adding 2wt% $\text{Ho}_{63.3}\text{Fe}_{36.7}$ to the magnet. Further, the coercivity increases by 123 kA/m (approximately 9.1%), the maximum magnetic energy product decreases from 290.94 kJ/m³ to 281.07 kJ/m³, and remanence decreases slightly. Through analysis of the microstructure and composition, it can be seen that the (Nd, Pr, Ho)₂Fe₁₄B shell layers form at the grain boundary, which enhances the coercivity of the magnet. X-ray diffraction analysis suggests that the diffraction peak intensity ratio of magnet $I_{(006)}/I_{(105)}$ increases from 0.92 to 1.32, which indicates that the alignment degree is improved and the influence on remanence is weakened. Therefore, regenerated magnets can possess improved coercivity while maintaining magnetic remanence.

Key words: NdFeB regenerated magnet; magnetic property; intergranular addition; alignment degree

NdFeB permanent magnet materials are largely used in the aerospace industry, medical and household devices due to their unconventional magnetic properties and low production cost^[1-4]. The production of NdFeB has increased steadily, the output of rare earth permanent magnet roughcast in China reaches 110 000 t in 2014 and continues to rise^[5,6], and it is predicted to increase to 120 000 t in 2020^[7]. However, the non-equilibrium exploitation of NdFeB permanent magnets severely restricts the long-term application of NdFeB resources.

Therefore, the search for a light rare earth replacement for Nd and the development of magnetic materials without rare earth elements have become a priority for scholars and industry. Unfortunately, substituting of Nd will reduce magnetic properties and cause vast work^[8-11]. However, a large amount of scrap materials will be formed during production and the replacement of downstream application apparatus.

According to the literature, shaping and processing of NdFeB result in approximately 15%~30% of the crude materials being wasted as scraps^[7,12-14]. Additionally, the percentage of rare earth scrap magnets is much higher than that of the initial ore^[15], and they cause less environmental contamination^[6,16,17]. Accordingly, recycling and reusing of NdFeB scrap magnets is an effective way to address the above concerns.

Many processes to treat NdFeB waste for the recovery of rare earth elements have been proposed. For instance, Lyman and Palmer^[18] reclaimed Nd by dissolving and reprecipitating scrap magnets in sulfuric acid. However, the process of depositing waste magnets will cause damage to the rare earth resources, and the sulfuric acid poses environmental risks. Hoogerstraete et al^[19] ground old NdFeB magnets into small granules for roasting, and then added HCl and HNO₃ for selective leaching. The extracted rare earth elements formed oxalate sediment through use of oxalic acid. However, the

Received date: December 12, 2020

Foundation item: National Key R&D Program of China (2016YFB0700901); National Natural Science Foundation of China (51761007); Science and Technology Project of Guangxi (2017AD23031); Science and Technology Plan Project of Fujian (18111010069)

Corresponding author: Yao Qingrong, Ph. D., Professor, Guangxi Key Laboratory of Information Materials, School of Materials Science and Engineering, Guilin University of Electronic Technology, Guilin 541004, P. R. China, E-mail: qingry96@guet.edu.cn

Copyright © 2021, Northwest Institute for Nonferrous Metal Research. Published by Science Press. All rights reserved.

generation of NdFeO₃ during the roasting process will suppress the leaching of the Nd element, resulting in a low recycling rate. Sasai and Shimamura^[14] introduced a mechanochemical means to reclaim rare earths from NdFeB waste magnets, achieving a recovery rate of 95%. However, the mechanochemical recycling method requires a treatment time of 6~24 h, which greatly affects the recovery availability of rare earth resources. Thus, in this work, a high-efficiency green physical method was used to clean the surface of the former NdFeB magnet, and then the secondary utilization of NdFeB was promoted through the addition of the Ho_{63.3}Fe_{36.7} alloy to the grain boundary.

1 Experiment

1.1 Preparation of NdFeB regenerated magnets

The composition of the waste magnet sample (from a Chinese company) is shown in Table 1. Both Ho and Fe metals with purity of 99.99% were used. Firstly, the surface of the waste magnet was polished by mechanical polishing and hydrogen crushed to create a coarse powder. Then, the coarse powder underwent jet-milling, resulting in a fine powder of 3~5 μm in size. Secondly, the Ho_{63.3}Fe_{36.7} alloy was prepared by arc-melting in an MSM20-7 melting furnace and turned over 4~5 times, and inserted into a quartz tube under an argon atmosphere. The alloy was annealed (600 °C) in a KSL-1200X gradient muffle furnace for 7 d. Next, the Ho_{63.3}Fe_{36.7} alloy was ground for 24 h using a QM-QX planetary ball mill (300 r/min) to obtain 2~4 μm particles. Finally, the waste particles and alloy particles were uniformly mixed according to the set proportion, and the mixture was subject to magnetic field press molding, followed by cold isostatic pressing. It was then sintered and annealed to obtain a regenerated NdFeB magnet.

1.2 Characterization

The magnet properties were tested using a NIM-10000H bulk rare earth permanent magnet nondestructive testing apparatus. The microstructure was observed using a Quanta 450FEG scanning electron microscope (SEM) with an electron backscatter diffractometer and equipped with an energy dispersive spectrometer (EDS); the regenerated magnet was analyzed in the range of 20°~90° with PL Xcel 3D X-ray diffraction (XRD). The density of NdFeB regenerated magnets was measured by electron density balance, based on the principle of drainage method.

2 Results and Discussion

2.1 XRD analysis

Fig. 1 shows the XRD patterns of regenerated magnets doped with various quantities of Ho_{63.3}Fe_{36.7} alloy powders. All diffraction peaks of the studied samples show a well texture in

(006), (004) and (008) except for the (105) diffraction peak. This indicates that the preferred alignment of the NdFeB regenerative magnet is in the (00L) direction. However, the appearance of the (105) diffraction peak is caused by the incomplete alignment of some main phase grains. Therefore, the ratio of the peak intensity of (006) and (105) is used to evaluate the alignment degree, which also affects the remanence of the magnet^[20]. Moreover, there are non-c-axis peaks in the XRD patterns of the Ho_{63.3}Fe_{36.7} alloy magnet, which may make the alignment of magnets difficult and affect the resulting alignment degree. As shown in Table 2, as the Ho_{63.3}Fe_{36.7} alloy addition increases from 0wt% to 2wt%, the value of $I_{(006)}/I_{(105)}$ increases from 0.92 to 1.32. By continuously increasing the amount to 3wt%, the value of $I_{(006)}/I_{(105)}$ decreases from 1.32 to 1.27. This can be attributed to the fact that Ho_{63.3}Fe_{36.7} alloy reduces the non-c-axis diffraction peaks in the magnet, which is beneficial to improve the alignment degree. Among them, 2wt% Ho_{63.3}Fe_{36.7} curve has the least impurity peaks, which can obtain the best alignment degree. Notably, the alignment deteriorates due to the increase of the liquid phase volume, leading to the decrease of $I_{(006)}/I_{(105)}$ with 3wt% Ho_{63.3}Fe_{36.7}.

2.2 SEM analysis

Fig. 2 shows SEM back-scattered micrographs of the regenerated magnets with different quantities of Ho_{63.3}Fe_{36.7}. The microstructure of the NdFeB regenerated magnet consists of white and gray contrasts. The white contrast corresponds to the Nd-rich phases of NdFeB, while the gray contrast corresponds to the main phase of Nd₂Fe₁₄B. As shown in Fig. 2a, in the magnet without Ho_{63.3}Fe_{36.7}, the white contrast Nd-rich phases of the regenerated magnet are block-dispersed and do not evolve into a continuous grain boundary phase.

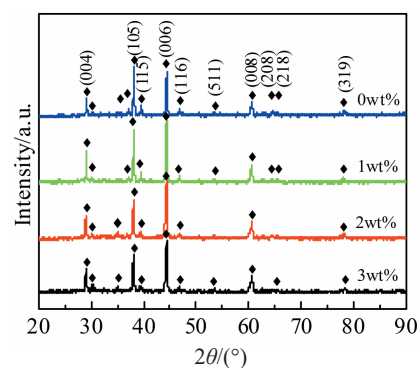


Fig.1 XRD patterns of the magnets with different quantities of Ho_{63.3}Fe_{36.7}

Table 2 Diffraction peak intensity of $I_{(006)}$ and $I_{(105)}$

Ho _{63.3} Fe _{36.7} content/wt%	$I_{(105)}$	$I_{(006)}$	$I_{(006)}/I_{(105)}$
0	2402	2220	0.92
1	2572	2846	1.10
2	2062	2721	1.32
3	2006	2554	1.27

Table 1 Chemical composition of NdFeB waste magnet (wt%)

Fe	Nd	Pr	B	Al	Cu
65.48	24.95	6.41	1.00	0.55	0.10

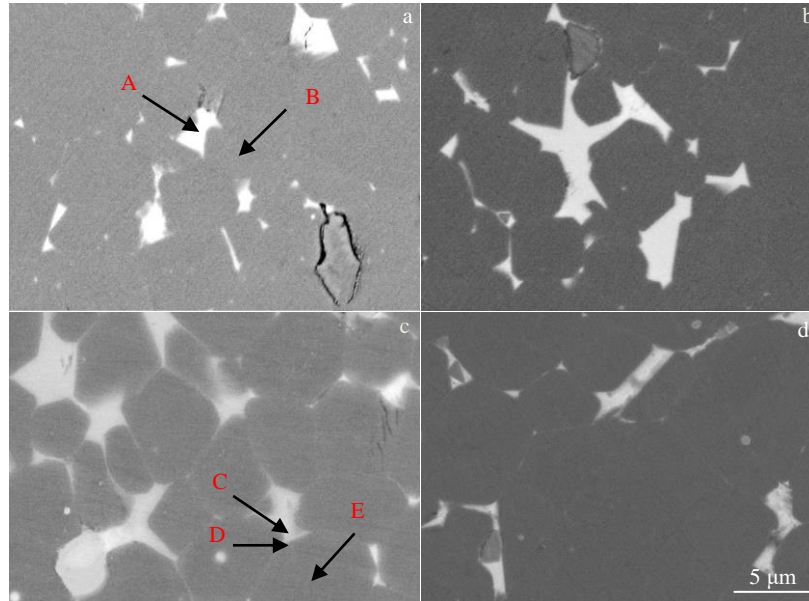


Fig. 2 SEM micrographs of the regenerated magnets with different additional quantities of $\text{Ho}_{63.3}\text{Fe}_{36.7}$: (a) 0wt%, (b) 1wt%, (c) 2wt%, and (d) 3wt%

This indicates that there are not enough Nd-rich phases during the liquid phase sintering process, leading to the direct contact with adjacent main phases and producing a coupling effect. In addition, the cracks in the magnet indicate poor wettability and binding force between the $\text{Nd}_2\text{Fe}_{14}\text{B}$ phase and intergranular phase^[3]. As shown in Fig. 2b~2d, with the intergranular addition of $\text{Ho}_{63.3}\text{Fe}_{36.7}$ alloy, the white contrast grain boundary phase distribution changes. With increasing the $\text{Ho}_{63.3}\text{Fe}_{36.7}$ content, the grain boundary phase changes from a block to a wide strip with some clear and continuous grain boundary phases, and it can be speculated that the wettability of the magnets increases^[21], and that the magnetic density is also improved, as reflected in Fig. 5. In comparison with the magnet with 1wt% $\text{Ho}_{63.3}\text{Fe}_{36.7}$, the intergranular Nd-rich phases become clearer and more continuous, which isolate the $\text{Nd}_2\text{Fe}_{14}\text{B}$ phase with 2wt% $\text{Ho}_{63.3}\text{Fe}_{36.7}$ addition, as shown in Fig. 2c. This is a result of the liquid phase sintering with $\text{Ho}_{63.3}\text{Fe}_{36.7}$ addition. Though the melting point of $\text{Ho}_{63.3}\text{Fe}_{36.7}$ (863 °C) is higher than that of the Nd-rich phase (665 °C)^[22,23], it is significantly lower than the sintering temperature (1072 °C). The $\text{Ho}_{63.3}\text{Fe}_{36.7}$ alloy and Nd-rich phase become liquid phases and mixed together at the sintering temperature, which increases the liquid phase volume of the magnet. Hence, there are sufficient Nd-rich phases to surround the $\text{Nd}_2\text{Fe}_{14}\text{B}$ phase grains and to form a continuous grain boundary phase during the sintering process. This also signifies that the adjacent ferromagnetic particles are well isolated, thus improving the magnet properties. Additionally, the alignment of the magnet is related to its microstructure. This grain boundary distribution can break the agglomeration of the main phase crystal grains, leading to easier magnet alignment. Hence, the number of non-orientation peaks is reduced so that the value

of the magnet $I_{(006)}/I_{(105)}$ increases from 0.92 to 1.32.

The influence of the distribution of Nd, Pr, Ho and Fe in the regenerated magnet on the magnetic properties was analyzed using EDS point-scan. Ho is neither found in the grain boundary phase, nor in the main phase of the magnet with 0wt% $\text{Ho}_{63.3}\text{Fe}_{36.7}$ (marked by points A and B in Table 3 and Fig. 2a). Table 3 summarizes the content of elements in the thick grain boundary layers (point C), the surface region close to the grain boundary layers (point D) and the main phase grain center (point E) in the case of 2wt% $\text{Ho}_{63.3}\text{Fe}_{36.7}$ addition. It can be seen that Ho is mainly concentrated in the thick grain boundary layers and diffused from the grain boundary phase to the $\text{Nd}_2\text{Fe}_{14}\text{B}$ phase. To further characterize the elemental distribution, EDS line-scan was used. As shown in Fig. 3, the EDS line-scan analysis indicates the graded distribution of Ho across the Nd-rich phases and the $\text{Nd}_2\text{Fe}_{14}\text{B}$ phase grains. It is found that Fe mainly exists in the $\text{Nd}_2\text{Fe}_{14}\text{B}$ phase, Pr and Nd are enriched in the grain boundary phase, and the Ho content gradually decreases from the intergranular phase to the central

Table 3 EDS spot scanning results of point A (grain boundary phase) and point B (center of the main phase) in Fig. 2a, and point C (thick grain boundary layers), point D (surface region close to the grain boundary layers) and point E (main phase grain center) in Fig. 2c (at%)

Point	Fe	Nd	Pr	Ho
A	0.39	70.59	29.02	0.00
B	86.36	11.12	2.52	0.00
C	60.19	25.91	7.84	2.17
D	79.69	13.13	3.69	1.51
E	84.28	10.87	2.64	0.40

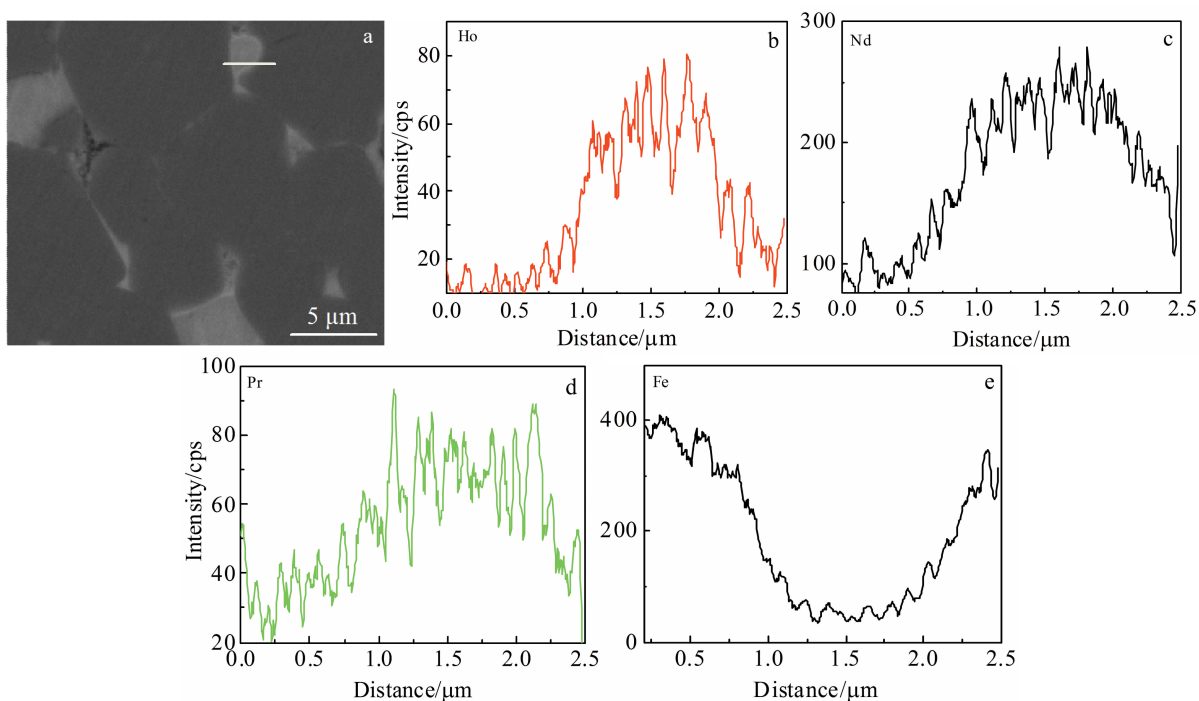


Fig.3 SEM image (a) and element EDS line-scan results of Ho (b), Nd (c), Pr (d) and Fe (e) across the intergranular phase and $\text{Nd}_2\text{Fe}_{14}\text{B}$ phase grains in regenerated magnets with 2wt% $\text{Ho}_{63.3}\text{Fe}_{36.7}$

area of the main phase. This is consistent with the results of the above point analysis. It can be explained that the diffusion of Ho from $\text{Ho}_{63.3}\text{Fe}_{36.7}$ to the $\text{Nd}_2\text{Fe}_{14}\text{B}$ phase causes Ho to replace part of Nd in the grain boundary layer during the sintering process, forming a $(\text{Nd, Pr, Ho})_2\text{Fe}_{14}\text{B}$ shell layer^[3,21,24].

2.3 Magnetic properties analysis

The magnetic properties of the regenerated NdFeB magnets with different quantities of $\text{Ho}_{63.3}\text{Fe}_{36.7}$ are shown in Fig.4. For the bare regenerated magnet, the coupling between the main phases is caused by the low volume fraction of the grain boundary phase, which reduces the coercivity of the magnet. When $\text{Ho}_{63.3}\text{Fe}_{36.7}$ content is increased from 0wt% to 2wt%, the coercivity (H_{cj}) is improved from 1352 kA/m to 1475 kA/m (increased by 9.1%). This is because the addition of $\text{Ho}_{63.3}\text{Fe}_{36.7}$ alloy forms a clear and continuous grain boundary phase between the adjacent main phases, so that the main phase no longer has a coupling effect, thereby improving the coercivity of the magnet. From the EDS results, it can be seen that Ho diffuses from the $\text{Ho}_{63.3}\text{Fe}_{36.7}$ to the $\text{Nd}_2\text{Fe}_{14}\text{B}$ phase and forms a $(\text{Pr, Nd, Ho})_2\text{Fe}_{14}\text{B}$ shell in the main phase boundary layer. Since the intrinsic anisotropy field H_A of $\text{Nd}_2\text{Fe}_{14}\text{B}$ ($H_A=5360$ kA/m) is lower than that of $\text{Ho}_2\text{Fe}_{14}\text{B}$ ($H_A=6000$ kA/m), the formation of $(\text{Pr, Nd, Ho})_2\text{Fe}_{14}\text{B}$ shell increases the H_A on the surface^[25,26]. Therefore, nucleation of the reverse domains external magnetic field can be prevented, which contributes to coercivity enhancement. With increasing the $\text{Ho}_{63.3}\text{Fe}_{36.7}$ addition amount to 3wt%, the coercivity (1477 kA/m) is increased only by 2 kA/m. This is because the addition of 3wt% $\text{Ho}_{63.3}\text{Fe}_{36.7}$ leads to the enrichment of the grain

boundary phase at grain boundary and the increase of grain size of main phase (Fig. 2d), which restrict the increase of coercivity of the magnet^[27,28].

As shown in Fig.4b and 4c, the remanence (B_r) is reduced from 1.22 T to 1.187 T and the maximum magnetic energy product $(BH)_{\text{max}}$ decreases from 290.94 kJ/m³ to 276.53 kJ/m³. This is because the magnetic polarization for $\text{Nd}_2\text{Fe}_{14}\text{B}$ is higher than of $\text{Ho}_2\text{Fe}_{14}\text{B}$, which can reduce the remanence. However, the remanence and maximum magnetic energy product slightly increase at 2wt% $\text{Ho}_{63.3}\text{Fe}_{36.7}$, which are 1.202 T and 281.07 kJ/m³, respectively. According to $B_r = A(1 - \beta) \frac{d_1}{d_2} \cos\theta J_s$ ^[29,30] (where d_1 is the actual density value and d_2 is the theoretical density value), the remanence of the magnet is primarily affected by the density of the magnet and the alignment degree of the main phase grain. It can be seen that there is a positive correlation between magnets density and remanence, that is, as the magnet density increases, remanence also increases. As shown in Fig. 5, with the addition of $\text{Ho}_{63.3}\text{Fe}_{36.7}$, the magnet density gradually increases, and it is optimal at 2wt% $\text{Ho}_{63.3}\text{Fe}_{36.7}$. Hence, the NdFeB regenerated magnet has the best alignment ($I_{(006)}/I_{(105)}=1.32$) and better density ($\rho=7.54$ g/cm³) at 2wt% $\text{Ho}_{63.3}\text{Fe}_{36.7}$ which can ameliorate the magnetic dilution caused by partial Ho replacement of Nd and slightly improve the remanence (B_r). As shown in Fig.4d, the NdFeB regenerated magnet displays the best comprehensive magnetic performance with the addition of 2wt% $\text{Ho}_{63.3}\text{Fe}_{36.7}$ [$(BH)_{\text{max}}+H_{\text{cj}}=1756.07$]. As mentioned above, 2wt% $\text{Ho}_{63.3}\text{Fe}_{36.7}$ addition can achieve the target of reducing tiny amount of remanent magnetism and

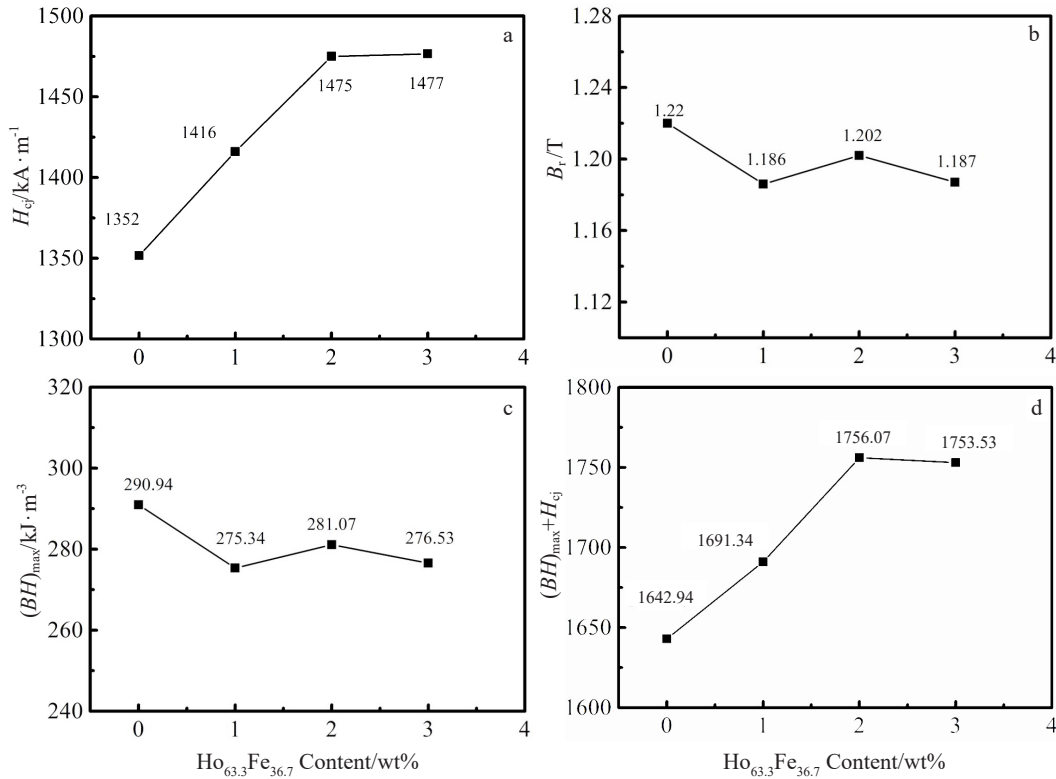


Fig.4 Magnetic properties of NdFeB regenerated magnets with different quantities of $\text{Ho}_{63.3}\text{Fe}_{36.7}$: (a) H_{cj} , (b) B_r , (c) $(BH)_{\text{max}}$, and (d) $(BH)_{\text{max}} + H_{cj}$

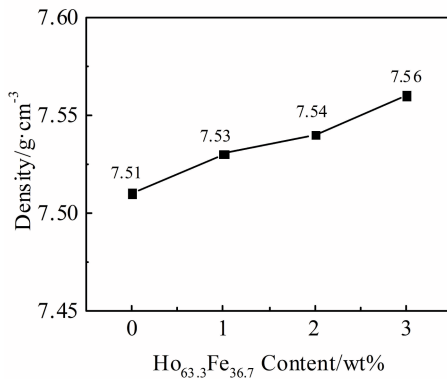


Fig.5 Magnet density with different $\text{Ho}_{63.3}\text{Fe}_{36.7}$ quantities

greatly improving the regenerative magnet of NdFeB.

3 Conclusions

1) The addition of $\text{Ho}_{63.3}\text{Fe}_{36.7}$ alloy to grain boundaries is a promising way to recycle the NdFeB waste magnets.

2) The NdFeB regenerated magnet displays the best comprehensive magnetic performance with addition of 2wt% $\text{Ho}_{63.3}\text{Fe}_{36.7}$. The coercivity improves from 1352 kA/m to 1475 kA/m, increased by 9.1%. While the remanence is reduced to 1.202 T and the maximum magnetic energy product decreases to 281.07 kJ/m^3 .

3) The addition of $\text{Ho}_{63.3}\text{Fe}_{36.7}$ alloy changes the distribution of the intergranular phases and forms continuous Nd-rich

phase. It can also decouple the neighboring ferromagnetic main phase. Furthermore, a $(\text{Pr}, \text{Nd}, \text{Dy})_2\text{Fe}_{14}\text{B}$ magnetically hardened shell forms after Ho diffuses into the $\text{Nd}_2\text{Fe}_{14}\text{B}$ phase grain surface, which improves magnetic coercivity and enhances the densification and the alignment degree of the regenerated magnets. The coercivity of the magnet is increased and the remanence is retained.

References

- 1 Sagawa M, Fujimura S, Togawa N et al. *Journal of Applied Physics*[J],1984, 55(6): 2083
- 2 Gutfleisch O, Willard M A, Bruck E et al. *Advanced Materials* [J], 2011, 23(7): 821
- 3 Liu X, Wang X, Liang L et al. *Journal of Magnetism and Magnetic Materials*[J], 2014, 370: 76
- 4 Jiang Q Z, Zhong M L, Quan Q C et al. *Journal of Alloys and Compounds*[J], 2016, 688: 363
- 5 Hu Z H, Qu H J, Zhao J Q et al. *Journal of Magnetism and Magnetic Materials*[J], 2014, 368: 54
- 6 Balaram V. *Geoscience Frontiers*[J], 2019,10(4): 1285
- 7 Kumari A, Sinha M K, Pramanik S et al. *Waste Management*[J], 2018, 75: 486
- 8 Li Aiwei, Feng Haibo, Huang Shulin et al. *IEEE Transactions on Magnetics*[J], 2015, 51(11): 2 103 603
- 9 Li Z, Liu W, Zha S et al. *Journal of Rare Earths*[J], 2015, 33(9): 961

- 10 Fang C C, Yao Q R, Xu Y Q et al. *Materials Science Forum*[J], 2018, 914: 73
- 11 Zhou Q Y, Liu Z, Guo S et al. *IEEE Transactions on Magnetics* [J], 2015, 51(11): 1
- 12 Chen H, Zhou S X, Dong B S et al. *Journal of Alloys and Compounds*[J], 2020, 819: 153 062
- 13 Jin H, Afiuny P, McIntyre T et al. *Procedia CIRP*[J], 2016, 48: 45
- 14 Sasai R, Shimamura N. *Journal of Asian Ceramic Societies*[J], 2018, 4(2): 155
- 15 Ferron C J, Henry P. *Canadian Metallurgical Quarterly*[J], 2016, 54(4): 388
- 16 Zamprogno Rebello R, Weitzel Dias Carneiro Lima M T, Yamane L H et al. *Resources, Conservation and Recycling*[J], 2020, 153: 104 557
- 17 Feng H, Zhang Y, Li A et al. *IEEE Transactions on Magnetics* [J], 2017, 53(11): 1
- 18 Lyman J W, Palmer G R. *High Temperature Materials and Processes*[J], 1993, 11(1-4): 175
- 19 Vander Hoogerstraete T, Blanpain B, Van Gerven T et al. *RSC Advance*[J], 2014, 4(109): 64 099
- 20 Lee Y I, Huang G Y, Shih C W et al. *Journal of Magnetism and Magnetic Materials*[J], 2017, 439: 1
- 21 Liang L P, Ma T Y, Zhang P et al. *Journal of Magnetism and Magnetic Materials*[J], 2014, 355: 131
- 22 Liang L, Ma T, Wu C et al. *Journal of Magnetism and Magnetic Materials*[J], 2016, 397: 139
- 23 Kaneko Y, Ishigaki N. *Journal of Materials Engineering and Performance*[J], 1994, 3: 228
- 24 Zhang X F, Guo S, Yan C J et al. *Journal of Applied Physics*[J], 2014, 115(17): 757
- 25 Hiroswawa S, Hitoshi K, Yamamoto H et al. *Journal of Applied Physics*[J], 1986, 59(3): 873
- 26 Kronmüller H, Durst K D. *Journal of Magnetism and Magnetic Materials*[J], 1988, 74: 291
- 27 Liu J, Sepehri-Amin H, Ohkubo T et al. *Acta Materialia*[J], 2015, 82: 336
- 28 Hono K, Sepehri-Amin H. *Scripta Materialia*[J], 2012, 67(6): 530
- 29 Kirchmayr H R. *Journal of Physics D: Applied Physics*[J], 1996, 29(11): 2763
- 30 Bezinge A, Braun H F, Muller J et al. *Solid State Commun*[J], 1985, 55: 131

晶界添加 $\text{Ho}_{63.3}\text{Fe}_{36.7}$ 对 NdFeB 再生磁体组织与性能的影响

孙前程¹, 姚青荣¹, 龙乾新¹, 黄伟超², 邓健秋¹, 王江¹, 饶光辉¹, 周怀营¹

(1. 桂林电子科技大学 材料科学与工程学院 广西信息材料重点实验室, 广西 桂林 541004)

(2. 中国稀土(广西)金源新材料有限公司, 广西 贺州 542603)

摘要: 采用一种高效、绿色的物理方法对 NdFeB 废旧磁体表面进行清理并回收利用。通过晶界添加低熔点 $\text{Ho}_{63.3}\text{Fe}_{36.7}$ 合金制备 NdFeB 再生磁体。在未添加 $\text{Ho}_{63.3}\text{Fe}_{36.7}$ 的磁体中, 没有足够的富 Nd 相隔离 $\text{Nd}_2\text{Fe}_{14}\text{B}$ 相, 从而导致磁体性能较差; 随着 $\text{Ho}_{63.3}\text{Fe}_{36.7}$ 合金的加入, 晶界相变得清晰且连续。在质量分数 2% $\text{Ho}_{63.3}\text{Fe}_{36.7}$ 添加量下, 钕铁硼再生磁体获得最佳磁性能 $[(BH)_{\text{max}} + H_{\text{cj}} = 1756.07]$ 。此时矫顽力增加 123 kA/m (约提高 9.1%), 磁体的最大能积由 290.94 kJ/m³ 下降到 281.07 kJ/m³, 而剩磁少量下降。通过对再生磁体显微组织和成分的分析可知, 磁体晶界处形成了 (Nd, Pr, Ho)₂Fe₁₄B 壳层, 这能够提高磁体的矫顽力。而 X 射线衍射分析表明, 磁体 $I_{(006)}/I_{(105)}$ 的衍射峰强度比从 0.92 提高到 1.32。这说明磁体取向度提高, 可以减弱对剩磁的影响, 从而使得再生磁体在保持剩磁的同时提高磁体的矫顽力。

关键词: NdFeB 再生磁体; 磁性能; 晶界添加; 取向度

作者简介: 孙前程, 男, 1992 年生, 硕士生, 桂林电子科技大学材料科学与工程学院, 广西 桂林 541004, E-mail: sunqc1215@163.com